PERGAMON

Carbon 38 (2000) 1437–1444

CARBON

The structure of near-spherical carbon nano-shells

J.M. Cowley[a,*], Ching-Hwa Kiang[b]

[a]*Department of Physics and Astronomy, Arizona State University, Tempe, AZ 85287-1504, USA*
[b]*Department of Chemistry and Biochemistry, University of California, Los Angeles, CA 90095-1569, USA*

Received 19 March 1999; accepted 25 October 1999

Abstract

The empty, near-spherical, carbon nanoshells, frequently observed in preparations of carbon nanotubes, have been studied using nanodiffraction with electron probes of diameter 1 nm or less, formed in a scanning transmission electron microscope, and STEM imaging. For the larger nanoshells, it is shown that the shell walls are made up of flat regions composed of successive layers of well-ordered graphitic structure, about 5 or 10 nm thick and mutually rotated about their common *c*-axis direction.

Keywords: A. Carbon clusters, Carbon nanotubes; C. Electron diffraction, STEM

1. Introduction

Near-spherical shells of graphitic carbon have been observed in electron microscope images for many years. These particles, having diameters varying from about 10 nm to 100 nm, may be hollow, with walls of thickness varying from about 5 nm to 50 nm, or they may be filled with metal, metal carbide or other materials. The walls are made of flat regions consisting of parallel graphene sheets, such as those in graphite, stacked with the typical 0.34-nm spacing. Fringes with the 0.34-nm spacing are visible in high-resolution electron microscope images in the wall areas where the incident beam is almost parallel to the sheets.

Heidenreich et al. [1] observed such particles in preparations of vacuum-evaporated carbon and suggested their use as a convenient test for microscope resolution and as a means for the calibration of magnification. Many observations of such near-spherical particles have been made, along with multi-walled, or single-walled, carbon nanotubes, for specimens prepared by use of carbon arcs in moderate-pressure inert gas atmospheres [2–7]. Similar nanoshells have been observed in specimens prepared by other methods. Frequently, when metals or metal compounds have been added to the anode of a carbon arc, small metal, metal carbide or metal oxide particles are seen to fill, or partially fill, graphitic shells similar to the empty carbon shells [5–10].

The mechanism for growth of such near-spherical shells is not known, except that, for the case of the filled shells, catalysed growth of the graphitic carbon on the crystals of the metals or metal compounds is suggested. The structures of the walls of the near-spherical shells have not been investigated in any detail. High-resolution electron microscopy shows that in the regions of the walls, the 0.34-nm fringes appear with varying contrast and often appear to be continuous around the corners between adjacent flat areas. In such imaged regions there are rarely any indications of variations of inter-planar spacing or other localised defects. There is rarely any interpretable contrast visible in the image areas where the incident beam passes through the middle of the hollow particles.

It appears to be generally assumed that the stacking of the graphitic planes within the flat regions of the walls of the particles is regular, as in graphite, with possible stacking disorders, probably at random. In this paper we report studies of the walls of such particles using nanodiffraction with an electron beam of diameter 1 nm or less obtained in a scanning transmission electron microscopy (STEM) instrument and the associated bright-field and dark-field STEM images. These studies provide evidence for a layering of the structure of the shells with changes in

*Corresponding author. Fax: +1-602-965-7954.
E-mail address: cowleyj@asu.edu (J.M. Cowley).

0008-6223/00/$ – see front matter
PII: S0008-6223(99)00272-9

the orientations of the layers occurring at fairly regular intervals.

2. Experimental methods

The near-spherical carbon shells have been observed in a variety of carbon preparations. In samples formed by the carbon-arc processes, or by other methods, the nano-shells, if empty, appear to be generally relatively small (20 to 100 nm in diameter, with walls 5 to 10 nm thick), as in Fig. 1a, but there are occasional larger particles with diameters of 100 nm or more and wall thicknesses up to 50 nm, as in Fig. 1b.

The samples were studied in a HB-5 STEM instrument from VG Microscopes Ltd. operating at 100 keV and fitted with two post-specimen lenses and a two-dimensional detector system so that the nano-diffraction patterns from any chosen portion of the STEM image can be viewed with a low-light-level TV camera or a CCD recorder array [11]. Nanodiffraction patterns are normally obtained with an electron beam having a convergence angle of about 4×10^{-3} radians and a beam diameter at the specimen of about 0.7 nm. Larger aperture sizes are sometimes used to give higher beam convergence angles and beam-diameters as small as 0.3 nm.

Nanodiffraction patterns may be recorded with the TV camera and a video-cassette recorder (VCR) to give 30 diffraction patterns per second. Series of patterns can be obtained while the incident beam is scanned along a line, or else scanned over an area of the image, so that the variations of structure over any chosen area of the speci-

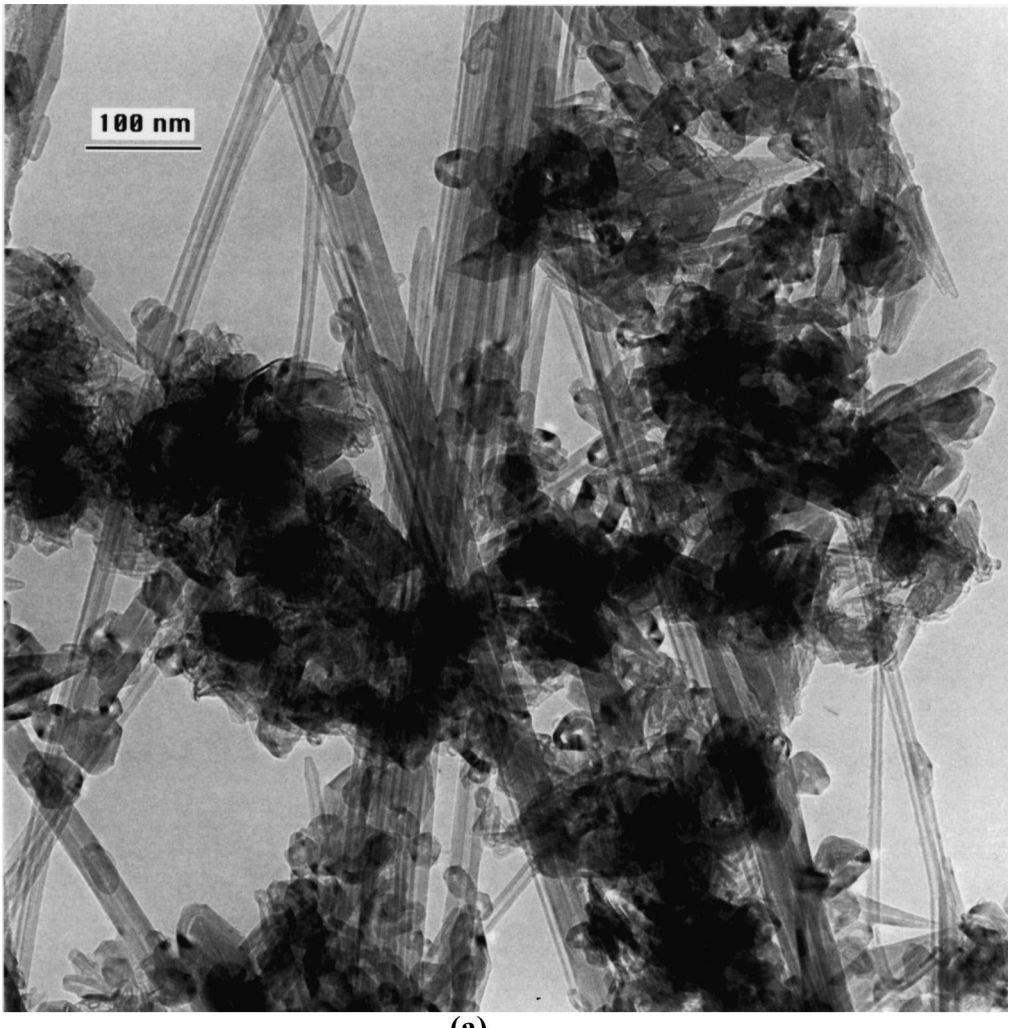

(a)

Fig. 1. (a) TEM image of multi-walled carbon nanotubes with nanoshells from a carbon-arc specimen. (b) STEM image of a large, irregular nanoshell, ~150 nm in diameter.

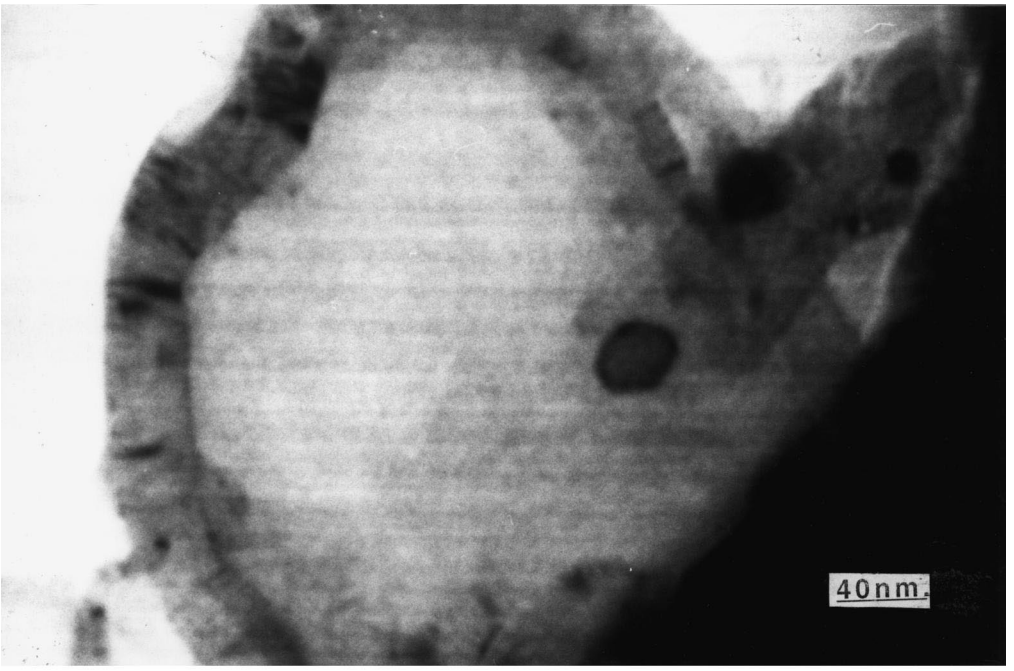

(b)

Fig. 1. (*continued*)

men may be examined. Alternatively, CCD recordings of very weak nanodiffraction patterns may be made with exposure times usually of about 1 s. Nano-diffraction patterns from various parts of shell-like carbon particles are shown in Fig. 3.

3. Observations

The images of Fig. 2 are STEM images obtained from portions of large nanoshells having diameters of about 200 nm and wall thicknesses of around 50 nm. The image, Fig. 2a, was obtained in the marginal bright-field/dark-field mode with the detector just on the edge of the central spot of the diffraction pattern in order to enhance the contrast of structural variations [12]. Fig. 2b is a more conventional dark-field STEM image, using diffracted beams other than those from the 0.34-nm layer spacing.

Nanodiffraction patterns were obtained from the various regions on the walls of the shells and from the regions within the shell images. Nano-diffraction patterns taken from the wall areas, such as Fig. 3a, show the clear, strong set of (00*l*) reflections corresponding to the 0.34-nm interplanar spacing. The parallel lines of (*hkl*) reflections sometimes show the spot positions corresponding to the graphite structure, but, more frequently, show spots distributed along the lines in a more complicated fashion, as in Fig. 3a. The distribution of spots on these lines is seen to vary rapidly as the incident beam is moved over the wall area.

The STEM images of the wall areas, Fig. 2a and b show some apparent faulting of the stacking of the carbon layers. There are bright lines, indicating local variations of the diffracted intensity, appearing at intervals of about 5 or 10 nm. It can be observed that the (*hkl*) lines in the nanodiffraction patterns, such as Fig. 3a, change as the beam is moved across these lines. The changes are consistent with changes in the orientation of the lattice which are azimuthal rotations of the lattice about the common graphitic *c*-axis.

Nano-diffraction patterns obtained with the beam passing through the central regions of the empty shells, such as Fig. 3b–d, show rings corresponding to the 1,0,0 and 1,1,0 reflections. These rings, coming from both the upper and the lower walls of the particle, are spotty, suggesting that a number of different orientations of the graphitic layers are present, rotated in azimuth about the *c*-axis with respect to each other.

For the thinner-walled shells, commonly found in the samples formed in carbon arcs, with wall thicknesses of the order of 5–10 nm, the number of spots on the rings is smaller. Sometimes, as in Fig. 3b, there are only two sets of six spots on each ring, corresponding to two single-crystal orientations, possibly one on the top side and one on the bottom side of the shell. For cases such as Fig. 3c and d there is evidence that six or more orientations are

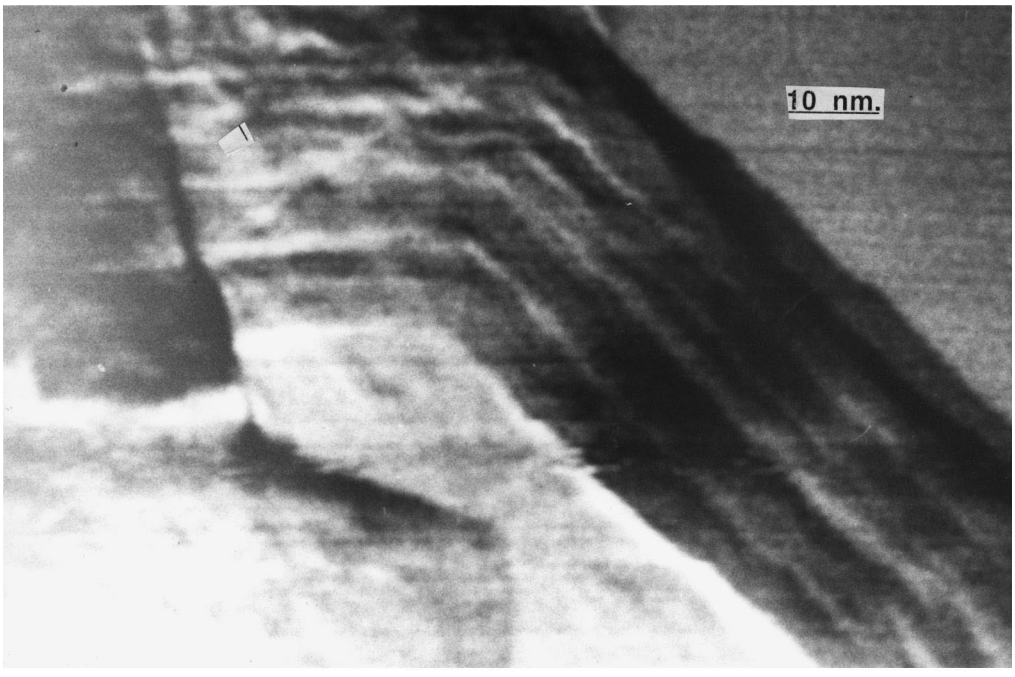

(a)

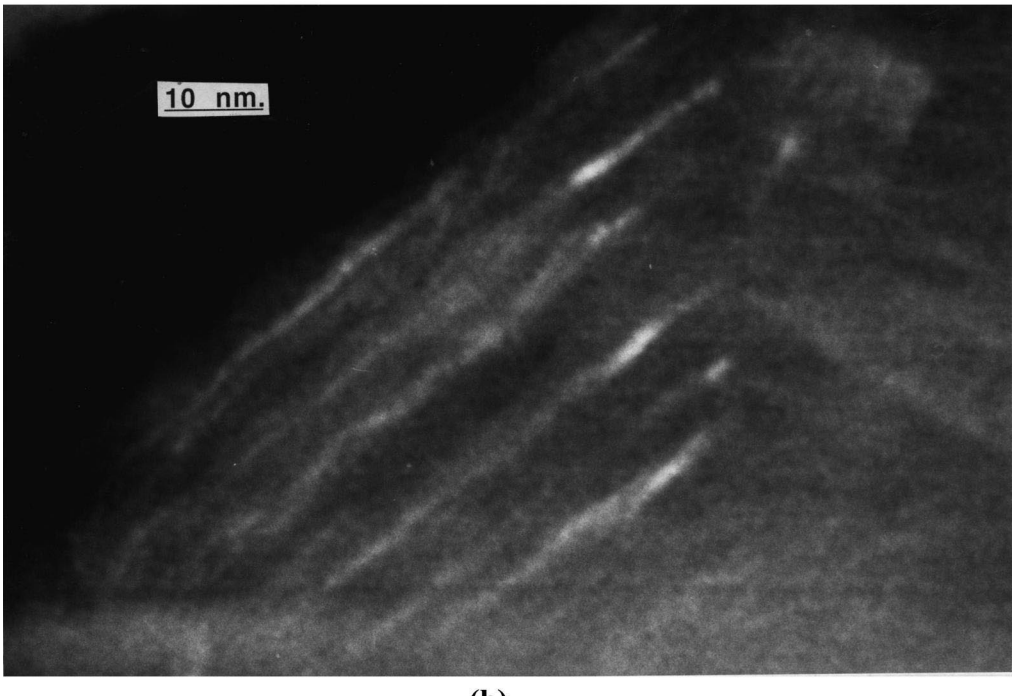

(b)

Fig. 2. (a) Dark-field/bright-field STEM image of part of the wall region of a large nanoshell. (b) Dark-field STEM image of a similar wall region showing lines of discontinuity, 5 or 10 nm apart.

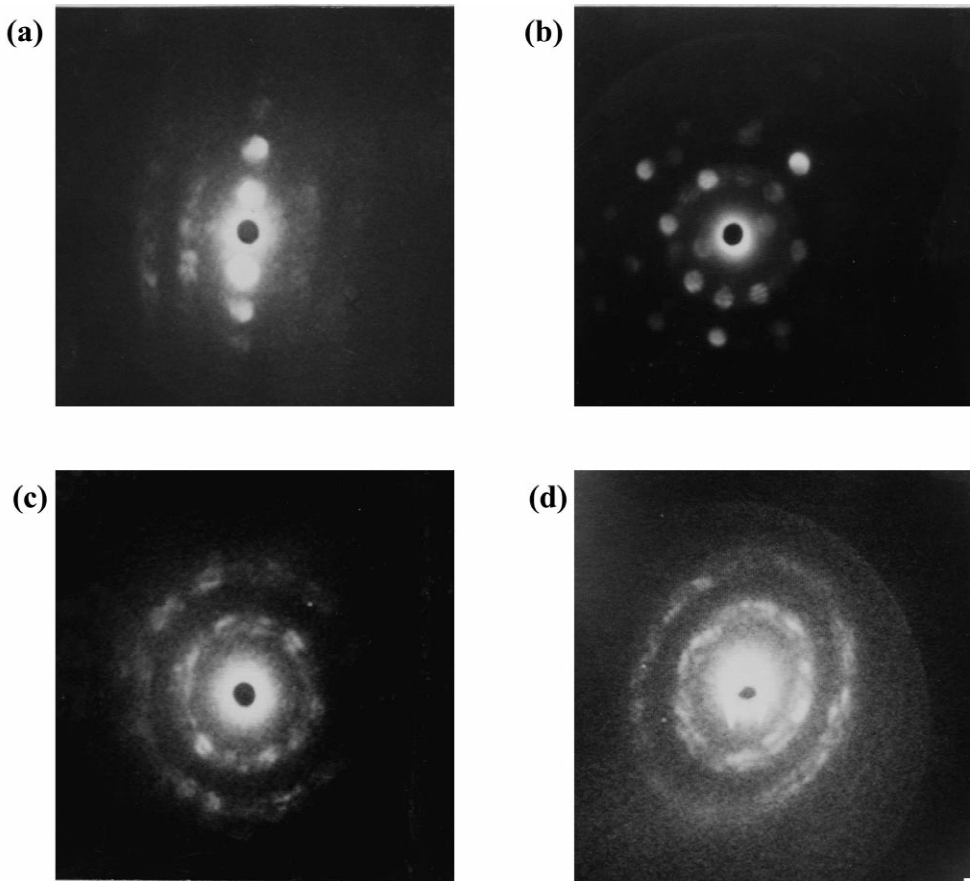

Fig. 3. (a) Nanodiffraction pattern from the wall region of a nanoshell. (b–d) Spotty ring patterns with the beam passing through the middle region of a nanoshell.

present, most orientations giving only two strong spots on a ring. This suggests that in these cases there are three or more orientations of the lattice on each of the top and bottom sides. This evidence indicates that the discontinuities in the wall structure, observed in Fig. 2a and b, correspond to changes in the azimuthal angle of the stacked carbon layers occurring at intervals of about 5 or 10 nm.

The diagram of Fig. 4 suggests the form of a cross-section of a typical nano-shell with a shell-wall thickness about 50 nm and the wall divided into, in this case, 10 flat regions. The lighter lines, separated by about 10 nm, represent the planes within each separate flat region on which the azimuthal rotation of the carbon layers takes place. These planar discontinuities are visible in Fig. 2a and b but are not usually visible in normal TEM or STEM bright-field images.

A further feature of the nano-diffraction patterns, Fig. 3c and d, is that the spots on the rings are clearly split into two or more components. In Fig. 3c, obtained with the beam almost perpendicular to the carbon sheets, most of the spots on the 1,0,0 ring are split radially into two components. Many of the spots on the 1,1,0, ring show three components. In Fig. 3d, the spotty rings are elliptical. Elliptical rings are formed from a disordered stacking of parallel sheet structures when the incident beam is tilted away from the normal to the plane of the sheets [13]. Most of the spots on the rings are split, as in Fig. 3c, although the splitting is not quite so consistent.

The splitting of the spots in these patterns has been attributed to the effect of the transmission of the incident beam through two crystals separated by a distance equal to the diameter of the shells [14]. The splitting corresponds to the imaging of the lattice of the first crystal by diffraction in the second crystal and provides an example of the ‘crystal atomic focuser’ effect [15], proposed and illustrated by computer simulations [16] as a method for obtaining ultra-high resolution in electron microscopy.

The boundaries where the ordered, single-crystal regions meet edge-on are expected to involve atomic configurations which are different from those of the ordered regions, possibly involving the local occurrence of pentagonal or

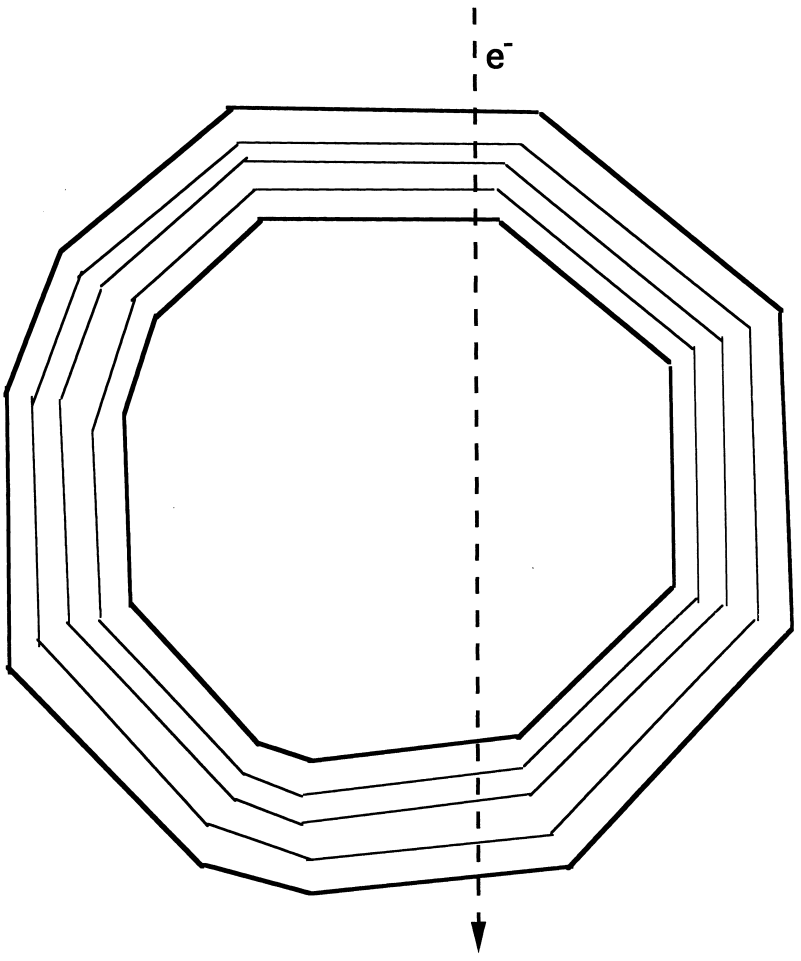

Fig. 4. Diagram suggesting the cross-section of a large nanoshell with wall thickness of about 35 nm. Thin lines are discontinuities between ordered regions.

heptagonal rings in place of the normal hexagonal carbon atom rings of the graphitic structure. These boundaries may therefore give diffraction intensities in other regions of the diffraction patterns than normal graphite. It is therefore possible to image such regions differentially by use of dark-field STEM imaging with particular detector configurations. Fig. 5, for example, obtained with a thin annular detector [12], set to pick up diffracted beams for spacings of around 0.15 nm, shows that within the region surrounded by the walls of the shell there are weak, rather diffuse boundary lines outlining areas 5 to 20 nm in diameter which presumably correspond to the ordered regions.

4. Conclusions

The evidence from the nano-diffraction patterns and the associated STEM images suggests that the walls of the carbon nano-shell particles have a more complicated structure than was previously expected.

The available evidence rules out any expansions or contraction of the dimensions within the carbon graphitic sheets or any bending or local defects within the ordered regions. It appears that the ordered regions within the shell walls have lateral dimensions of 5 to 20 nm and thicknesses of around 5 nm or 10 nm. Within the walls of the larger shells a number of such regions may be stacked with apparently random relative azimuthal rotations about the common *c*-axis. At the edges of the ordered regions, adjacent ordered regions meet with a difference in orientation of some 30 to 60 degrees between the normals to the planes. As suggested in Fig. 4 and seen in Fig. 2, the change in orientation takes place on common radial planes for all radially stacked layers. It may well be that the junctions between the ordered regions, forming with well-defined boundary planes, result from simple considerations of minimizing the strain fields.

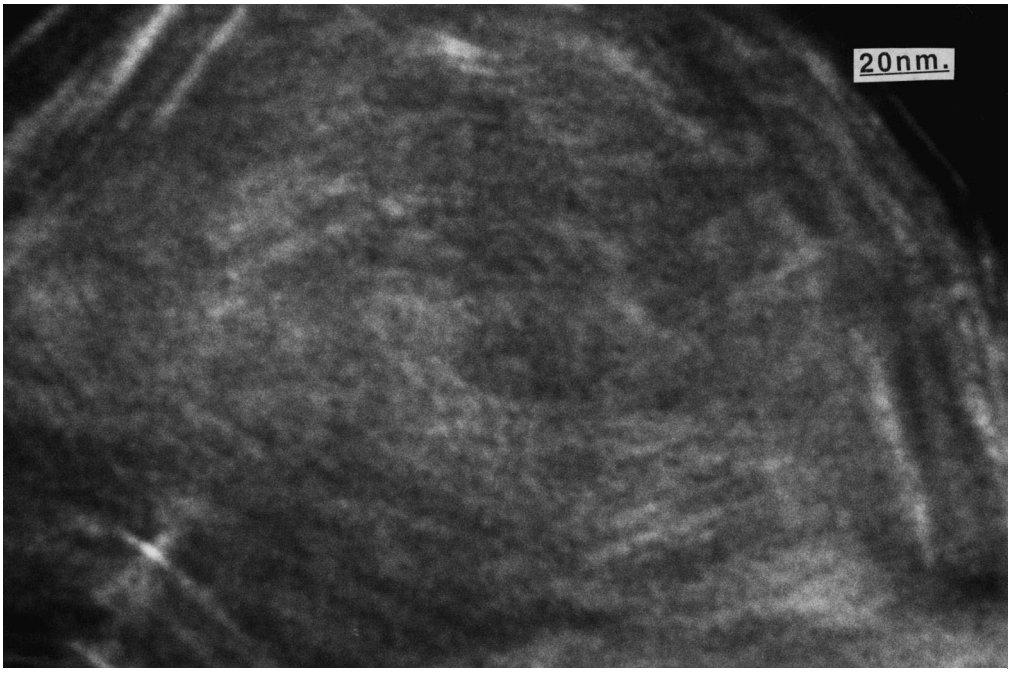

Fig. 5. Dark-field STEM image of a large nanoshell, showing weak contrast indicating the boundaries between ordered domains.

For the specimens formed by carbon-arc methods most of the carbon nano-shell particles are small, with diameters and wall thicknesses smaller than those of Fig. 2, so that the number of discontinuities where the carbon layer lattice rotates is less and the distances between the tilt discontinuities are also smaller.

The mechanism by which the empty carbon nano-shells are formed remains unresolved. However, it is difficult to imagine that the formation of such structures, with the twisted stacks of highly ordered crystalline regions, meeting at their edges with a relative tilt 30 to 60 degrees, could take place except by growth around some metallic or other solid particles. It is suggested that, after the shells have been formed in this way, the internal particles evaporate, leaving the carbon nano-shells empty. The observations of partially-filled shells [5–10] appears to support this view.

Acknowledgements

This work made use of the facilities of the ASU Center for High Resolution Electron Microscopy. C.H.K. thanks the support of the UC Energy Institute.

References

[1] Heidenreich RD, Hess WM, Ban LL. A test object and criteria for HREM. J Appl Cryst 1968;1:1–7.

[2] Ando Y, Iijima S. Preparation of carbon nanotubes by arc-discharge evaporation. Jpn J Appl Phys 1993;32:L107–109.

[3] Seraphin S, Zhou D, Jiao J. Extraordinary growth phenomena in carbon nanoclusters. Acta Microscopica 1994;3:45–64.

[4] Bethune DS, Kiang C-H, de Vries DS, Gorman G, Savoy R, Vasquez J, Beyers R. Cobalt-catalysed growth of carbon nanotubes with single-atomic-layer walls. Nature 1993;363:605–6.

[5] Kiang C-H, Goddard III WA, Byers R, Salem JR, Bethune DS. Catalytic synthesis of single-layer carbon nanotubes with a wide range of diameters. J Phys Chem 1994;98:6612–8.

[6] Kiang C-H, Dresselhaus MS, Beyers R, Bethune DS. Vapor-phase self-assembly of carbon nanomaterials. Chem Phys Lett 1996;259:41–7.

[7] Kiang C-H, Goddard III WA, Beyers R, Bethune DS. Carbon nanotubes with single-layer walls. Carbon 1995;33(7):903–14.

[8] Liu M, Cowley JM. Encapsulation of lanthanum carbide in carbon nanotubes and carbon nanoparticles. Carbon 1995;33(2):225–32.

[9] Seraphin S, Zhou D, Jian J, Withers JC, Routfy J. Yttrium carbide in nanotubes. Nature 1993;362:503.

[10] Cook J, Sloan A, Chu A, Heesom R, Green MLH, Hutchison JL, Kawasaki M. Identifying materials incorporated into carbon nanotubes by HREM and microanalysis. JEOL News 1996;32E:2–5.

[11] Cowley JM. Electron nanodiffraction: progress and prospects. J Electron Microsc 1996;45:3–10.

[12] Cowley JM. Configured detectors for STEM imaging of thin specimens. Ultramicroscopy 1993;49:4–13.

[13] Schiffmaker G, Dexpert H, Caro P, Cowley JM. Elliptical

electron diffraction patterns from ‘turbostratic’ graphite. J Microscopie Spectros Electronique 1980;5:729–34.
[14] Cowley JM. Atomic-focuser imaging in electron nanodiffraction from carbon nanoshells. Ultramicroscopy (in press).
[15] Cowley JM, Spence JCH, Smirnov VV. The enhancement of electron microscope resolution by use of atomic focusers. Ultramicroscopy 1997;68:135–48.
[16] Cowley JM, Dunin-Borkowski RE, Hayward M. The contrast of images formed by atomic focusers. Ultramicroscopy 1998;72:223–32.